Int. J. Heat Mass Transfer. Vol. 26, No. 8, pp. 1159–1171, 1983
Printed in Great Britain

0017–9310/83 $3.00 + 0.00

HYDRODYNAMIC AND HEAT TRANSFER ANALYSIS OF TWO-PHASE ANNULAR FLOW WITH A NEW LIQUID FILM MODEL OF TURBULENCE

FLAVIO DOBRAN
Stevens Institute of Technology, Hoboken, NJ 07030, U.S.A.

(*Received* 8 *February* 1982 *and in final form* 9 *December* 1982)

Abstract—A new method is presented for the analysis of hydrodynamics and heat transfer of two-phase annular flows with turbulent liquid films. Based on the experimental observation, the liquid film in two-phase annular flow is divided into a continuous layer adjacent to the channel surface and into a wavy layer close to the liquid–gas interface. In the continuous liquid layer region of the film, it is argued that the turbulence structure is similar to the structure of single phase turbulent pipe flow, and in the wavy layer region of the film, it is assumed that the eddy diffusion length is proportional to the thickness of this region. Experimental data in upflow and downflow confirmed the validity of the basic assumption of the turbulent structure in the film, and revealed the value for the wavy layer momentum diffusivity. This diffusivity is found to have a lower value than in the single phase pipe flow at the equivalent distances from the channel wall. The two-layer liquid film structure is integrated into an analysis for the prediction of hydrodynamics and heat transfer in annular two-phase flows. Analytic results are compared to the results of other analytical models and to the experimental data in upflow, downflow and horizontal flow. In all cases considered, very good comparison is achieved in both hydrodynamics and heat transfer.

NOMENCLATURE

A, flow cross-sectional area;
Bo, buoyancy number, $1-\rho_g/\rho_l$;
Cp, specific heat at constant pressure;
$D; D^+$, tube internal diameter; $\rho_l D u^*/\mu_l$;
f, friction factor;
g, gravitational constant;
h, heat transfer coefficient;
h_{lg}, enthalpy of evaporation;
k, thermal conductivity;
N_l, two-phase Grashof number, $(gD^3\rho_l(\rho_l-\rho_g)/\mu_l^2)^{1/2}$;
Nu_δ, Nusselt number, $h\delta/k_l$;
Pr, Prandtl number, $\mu Cp/k$;
Pr_{eff}, effective Prandtl number for the wavy layer region of the film, $\mu_{eff}/\rho_l\varepsilon_{eff}$;
Pr_{lt}, turbulent Prandtl number for the continuous layer region of the liquid film, $\varepsilon_m/\varepsilon_h$;
q, heat flux;
Re_c, gas core Reynolds number, $u_c\rho_c D/\mu_g$;
Re_l, film Reynolds number, $4W^+$;
S_l, subcooling number, $Cp_l(T_{sat}-T_w)/h_{lg}$;
$T; T^+$, temperature; $Cp_l\rho_l u^*(T_w-T)/q_w$;
$u; u_c$, axial film velocity; superficial gas velocity, $A_c u_g/A$;
u^*, shear velocity, $(|\tau_w|/\rho_l)^{1/2}$;
u^+, dimensionless film velocity, u/u^*;
W^+, dimensionless film flow-rate, $\int_0^{\delta^+} u^+\,dy^+ = Re_l/4$;
$y; y^+$, distance from the channel wall; $\rho_l u^* y/\mu_l$.

Greek symbols

α_c, gas core void fraction, $A_g/(A_g+A_d)$;
β, interfacial shear stress parameter, defined by equation (23);
$\delta; \delta^+$, film thickness; $\rho_l\delta u^*/\mu_l$;
$\delta_c; \delta_c^+$, wave crests thickness; $\rho_l\delta_c u^*/\mu_l$;
$\delta_t; \delta_t^+$, continuous liquid layer thickness; $\rho_l\delta_t u^*/\mu_l$;
$\delta_v; \delta_v^+$, viscous sublayer thickness; $\rho_l\delta_v u^*/\mu_l$;
$\varepsilon_m; \varepsilon_h$, turbulent diffusivities for momentum and heat;
$\mu; \nu$, viscosity; μ/ρ;
ρ, density;
τ, shear stress.

Subscripts

c, pertains to the core;
d, pertains to liquid droplets in the core;
eff, effective;
g, pertains to the gas phase;
i, liquid film–gas core interface;
l, pertains to the liquid phase;
sat, saturation value;
w, wall.

1. INTRODUCTION

TWO-PHASE annular flow patterns occur in many process and power generating systems. The liquid flows adjacent to the channel wall, and the gas or vapor flows in the channel core with entrained liquid droplets. At low gas and liquid velocities the gas–liquid interface is smooth and stable. At increasing gas velocities the interface becomes covered with 2- and 3-dim. waves and large amplitude roll waves [1]. Very high gas velocities produce breakdown of these waves and the entrainment of liquid droplets in the gas core. The topological structure of the waves is very similar in horizontal and vertical flow orientations [2].

1.1. *Previous work*

The presence of waves on the interface of liquid film and gas core in two-phase annular flow produces a different turbulence structure in the film from that in single phase pipe flow and external boundary layer flow. Air–water experiments of Chien and Ibele [3], Ueda and Tanaka [4], and Ueda and Nose [5] indicate that the liquid film can be divided into two layers: the continuous liquid layer of thickness δ_t, and into a disturbed wavy layer of thickness $(\delta_c - \delta_t)$, as is shown in Fig. 1. The continuous layer is a region close to the wall of the channel which is for most of the time covered by the liquid. δ_c is the thickness of wave crests, and δ is the liquid film thickness.

In the past the analytic modeling of turbulence in the liquid film has been carried out as in single phase flow. Thus, Dukler [6] for downflow, and Hewitt [7] for upflow, utilized Deissler's eddy diffusivity for $y^+ \leqslant 20$, and Von Karman's eddy diffusivity for $y^+ > 20$ to find the turbulent velocity distribution in the film. Davis *et al.* [8] utilized the above eddy diffusivities to study hydrodynamics and heat transfer in the horizontal stratified flow, and Goss *et al.* [9] modified the Von Karman constant in the Van Driest model for the eddy diffusivity to account for the liquid–gas interface shear stress. Yet another turbulence model by Butterworth [10] utilizes the universal velocity profile of single phase flow to describe the heat and momentum transport in the liquid film.

In contrast to the above turbulence models which allow for an increase of effective momentum and heat transport from the wall of the channel towards the edge of the liquid film, Blangetti and Schlunder [11] allow for the decrease of eddy diffusivity near the liquid film–gas core interface. This diffusivity model, first proposed by Levich [12], is found reasonable for the description of gas absorption into the falling turbulent liquid films [13] in the absence of surface waves.

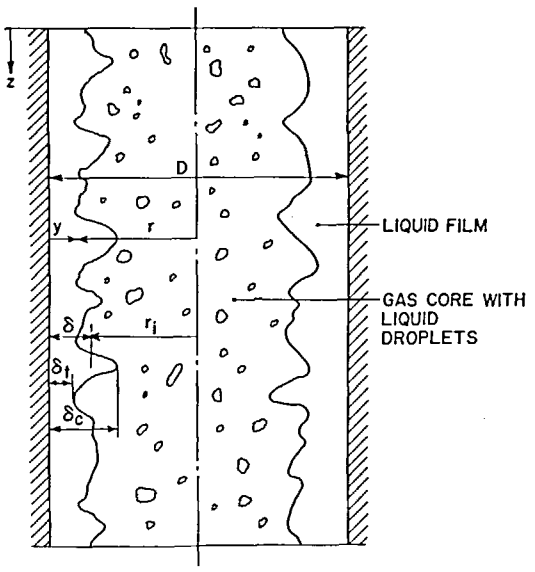

FIG. 1. Representation of continuous layer thickness δ_t, wavy layer thickness $(\delta_c - \delta_t)$, and film thickness δ in two-phase annular flow.

The eddy diffusivity models of Deissler, Von Karman and Van Driest yield hydrodynamic and heat transfer results that are similar to the results when the universal velocity profile is utilized [4, 5, 14]. Comparison of these theoretical models with the experimental data in turbulent film flow indicates that for identical values of the film Reynolds numbers and interfacial shear stress parameters β, the theories give thicker films and overpredict the heat transfer rate through the liquid film. The overprediction of the heat transfer rate is credited to the low value of the eddy diffusivity near the liquid film–gas core interface which is not accounted for in these models. When account is taken of the decrease in the eddy diffusivity near the interface [11] by utilizing the model of Levich, the heat transfer rate is underpredicted. This is of no surprise since the eddy diffusivity model of Levich does not account for the presence of waves on the interface of the liquid film.

The above conclusions suggest the inadequacy of the available eddy diffusivity models for modeling turbulence in the liquid film of two-phase flows, and clearly indicate that the turbulence structure of the film is different from the single phase pipe flow and the external boundary layer flow. Any improvement in the theory can, therefore, be achieved only if such a difference is recognized.

1.2. *Objectives of the paper*

The paper has the following objectives:

(1) To propose a novel turbulence model for the liquid film. In the continuous layer region of the liquid film, the turbulence structure is assumed to be similar to the single phase turbulent flow, and, in the wavy layer region of the film, the effective momentum and heat diffusivities are assumed to depend on the thickness of the wavy layer.

(2) To show how the wavy layer effective diffusivity can be ascertained from the experimental data.

(3) To incorporate the two-layer film structure into hydrodynamic and heat transfer models for the two-phase annular flow.

(4) To compare the predictions of the models with predictions of existing models and with the experimental data in upflow, downflow, and horizontal flow.

(5) To illustrate that the present theory predicts the experiments very well for a wide range of flow conditions in turbulent film flow.

2. ANALYSIS

2.1. *Turbulence model for the liquid film*

A state of the liquid film is illustrated in Fig. 1. It consists of a continuous liquid layer region of thickness δ_t, and a wavy layer region of thickness $(\delta_c - \delta_t)$. For the turbulent momentum and heat diffusion in the film, it is assumed that they are caused by the gradients of

the mean velocity and temperature fields and by the characteristic length scales of different regions in the film. This assumption is plausible in view of the forced convective nature of the flow field.

In the continuous layer region of the liquid film, the turbulent momentum diffusion is governed by the conditions near the channel wall. In this region, the effective momentum diffusivity should have a similar structure as in single phase pipe flow, i.e.

$$(\mu_{\text{eff}})_c = \mu_{\text{eff}}(\rho_l, \mu_l, |\tau_w|, y). \tag{1}$$

In the wavy layer region of the film, the turbulent diffusion distance (or eddy size) should be proportional to the thickness of the wavy layer ($\delta_c - \delta_t$) rather than to the distance from the channel wall—at least in a first order approximation. Other relevant parameters which can affect the effective diffusivity in the wavy layer region are the wall shear stress, some suitable measure of deviation of the interfacial shear stress from the wall shear stress, surface tension which can affect the damping of eddies near the interface, and the gravitational body force. In the present paper, I have invoked the simplest representation for the wavy layer region turbulence structure as follows:

$$(\mu_{\text{eff}})_{wl} = \mu_{\text{eff}}(\rho_l, \mu_l, |\tau_w|, \delta_c - \delta_t). \tag{2}$$

Dimensional analysis of equations (1) and (2) yields, respectively,

$$\left(\frac{\mu_{\text{eff}}}{\mu_l}\right)_c = f_1(y^+), \tag{3}$$

$$\left(\frac{\mu_{\text{eff}}}{\mu_l}\right)_{wl} = f_2(\delta_c^+ - \delta_t^+) \tag{4}$$

where $y^+ = \rho_l u^* y/\mu_l$ is the nondimensional distance from the channel wall, and $u^* = (|\tau_w|/\rho_l)^{1/2}$ is the shear velocity.

In the continuous layer region of the film, the functional relationship in equation (3) can be that of Deissler, Van Driest, Prandtl, and others. Here the Prandtl relationship is used, i.e.

$$(\mu_{\text{eff}}/\mu_l)_c = 1 \quad \text{in the viscous sublayer, and} \tag{5}$$

$$(\mu_{\text{eff}}/\mu_l)_c = Ky^+ \quad \text{in the turbulent layer.} \tag{6}$$

2.2. *Velocity profile in the continuous layer region of the film*

The velocity profile in the continuous layer region of the film follows from the usual relation for thin liquid films,

$$\tau = \mu_{\text{eff}} \frac{\partial u}{\partial y} \tag{7}$$

where u is the average axial velocity. Since the continuous layer thickness rapidly decreases with increasing gas velocity or interfacial shear stress (see below), it is permissible to set $\tau = \tau_w$ in equation (7) and integrate by utilizing equations (5) and (6). This procedure gives the usual relations of single phase turbulent flow,

$$u^+ = y^+, \quad \text{for } y^+ \leqslant \delta_v^+, \tag{8}$$

$$u^+ = \frac{1}{K} \ln y^+ + A, \quad \text{for } y^+ > \delta_v^+ \tag{9}$$

where $\delta_v^+ = \rho_l \delta_v u^*/\mu_l$, and $u^+ = u/u^*$ is the dimensionless film velocity. The accurate knowledge of the viscous sublayer thickness δ_v^+ and of the constants A and K must await future experimental measurement of the velocity profile in the film. At the present time, the most reasonable representation of the velocity profile in equations (8) and (9) is that of the single phase flow universal profile, i.e.

$$\delta_t^+ \leqslant 5; \quad u^+ = y^+, \quad \text{for } y^+ \leqslant \delta_t^+ \equiv \rho_l \delta_t u^*/\mu_l, \tag{10}$$

$$5 < \delta_t^+ \leqslant 30; \quad u^+ = y^+, \quad \text{for } y^+ \leqslant 5,$$
$$u^+ = -3.05 + 5 \ln y^+, \quad \text{for } 5 < y^+ \leqslant \delta_t^+, \tag{11}$$

$$\delta_t^+ > 30; \quad u^+ = y^+, \quad \text{for } y^+ \leqslant 5,$$
$$u^+ = -3.05 + 5 \ln y^+, \quad \text{for } 5 < y^+ \leqslant 30,$$
$$u^+ = 5.5 + 2.5 \ln y^+, \quad \text{for } 30 < y^+ \leqslant \delta_t^+. \tag{12}$$

2.3. *Velocity profile in the wavy layer region of the film*

In the wavy layer region of the liquid film, the effective momentum diffusivity is expressed by equation (4). The distribution of shear stress in this region is most simply obtained for thin liquid films by ignoring the inertia forces (but not gravity and pressure gradient forces) in the turbulent momentum equation for the film, i.e.

$$\frac{\tau}{\tau_w} = 1 - \left(1 - \frac{\tau_i}{\tau_w}\right) \frac{y^+}{\delta^+} \tag{13}$$

where τ_i is the shear stress at the liquid–gas interface. Substituting for τ from equation (7) into equation (13), and integrating from $y^+ = \delta_t^+$ to $y^+ > \delta_t^+$, yields the wavy layer turbulent velocity distribution

$$u^+ = u^+(\delta_t^+) + \frac{(y^+ - \delta_t^+)}{\left(\frac{\mu_{\text{eff}}}{\mu_l}\right)_{wl}} \times \left[1 - \left(1 - \frac{\tau_i}{\tau_w}\right) \frac{y^+ + \delta_t^+}{2\delta^+}\right] \tag{14}$$

where $u^+(\delta_t^+)$ is computed from equations (10)–(12).

The dimensionless mass flow-rate W^+ follows from equations (10)–(12) and (14), i.e.

$$W^+ = \frac{Re_l}{4} = \int_0^{\delta^+} u^+ \, dy^+ = W^+(\delta_t^+) + (\delta^+ - \delta_t^+) \times \left\{ u^+(\delta_t^+) + \frac{(\delta^+ - \delta_t^+)}{2\left(\frac{\mu_{\text{eff}}}{\mu_l}\right)_{wl}} \left[1 - \left(1 - \frac{\tau_i}{\tau_w}\right) \frac{\delta^+ + 2\delta_t^+}{3\delta^+}\right] \right\}. \tag{15}$$

Re_l is the film Reynolds number, and

$\delta_t^+ \leqslant 5$;

$$u^+(\delta_t^+) = \delta_t^+,$$
$$W^+(\delta_t^+) = \tfrac{1}{2}(\delta_t^+)^2, \tag{16}$$

$5 < \delta_t^+ \leqslant 30$;

$$u^+(\delta_t^+) = -3.05 + 5 \ln \delta_t^+, \tag{17}$$
$$W^+(\delta_t^+) = 5\delta_t^+ \ln \delta_t^+ - 8.05\delta_t^+ + 12.51,$$

$\delta_t^+ > 30$;

$$u^+(\delta_t^+) = 5.5 + 2.5 \ln \delta_t^+, \tag{18}$$
$$W^+(\delta_t^+) = 2.5\delta_t^+ \ln \delta_t^+ + 3\delta_t^+ - 64.$$

2.4. *Evaluation of the wavy layer momentum diffusivity*

Equation (15) allows us to test the validity of the wavy layer turbulence structure as expressed by equation (2), since from the experimental information of $W^+, \delta^+, \delta_t^+$, δ_c^+ and τ_i/τ_w, equation (15) can be solved for $(\mu_{eff}/\mu_l)_{wl}$. The available experimental studies in the literature are very few indeed which allow the extraction of the above information on the distribution of $(\mu_{eff}/\mu_l)_{wl}$. These are the air–water (adiabatic) downflow experiments of Chien and Ibele [3] in a 0.0508 m diameter tube, and air–water (adiabatic and non-adiabatic) downflow and upflow experiments of Ueda *et al.* [4, 5] in a 0.0288 m diameter tube.

In the experimental studies of refs. [3–5], the continuous liquid layer thickness δ_t has a remarkably simple expression in the sense that δ_t primarily depends on the gas core Reynolds number and on the tube diameter. Figure 2 illustrates the experimental observations where different tube diameter data of refs. [3–5] have been scaled by the parameter N_1. This parameter represents the ratio of gravity to viscous forces and appears more visibly in the analysis below. Although slight differences exist in the distribution of δ_t in upflow, downflow, and between different investigators in downflow, I have chosen to represent all sets of data in Fig. 2 by an average representation for the continuous liquid layer thickness as follows:

$$\frac{\delta_t^+}{D^+} = 140 N_1^{0.433} Re_c^{-1.35} \tag{19}$$

where $N_1 = (gD^3\rho_l(\rho_l - \rho_g)/\mu_l^2)^{1/2}$, $Re_c = u_c\rho_c D/\mu_g$, u_c is the superficial velocity of gas and ρ_c is the homogeneous density of the core. This representation is valid for $1.5 \times 10^4 < Re_c < 1.5 \times 10^5$ in upflow, downflow, and apparently for different tube diameters. The experiments of Chien and Ibele [3] show weaker dependence of δ_t on the gas Reynolds number than the experiments of Ueda *et al.* [4, 5], and the latter experiments in downflow show that below $Re_c \cong 1.5 \times 10^4$, δ_t levels off to a constant value. These observations should be more clearly substantiated in future experiments and integrated into a more complete model for the continuous liquid layer thickness distribution.

The experimental data in Fig. 2 clearly illustrate that the liquid–gas interface friction has the effect of greatly influencing the thickness of continuous liquid layer δ_t,

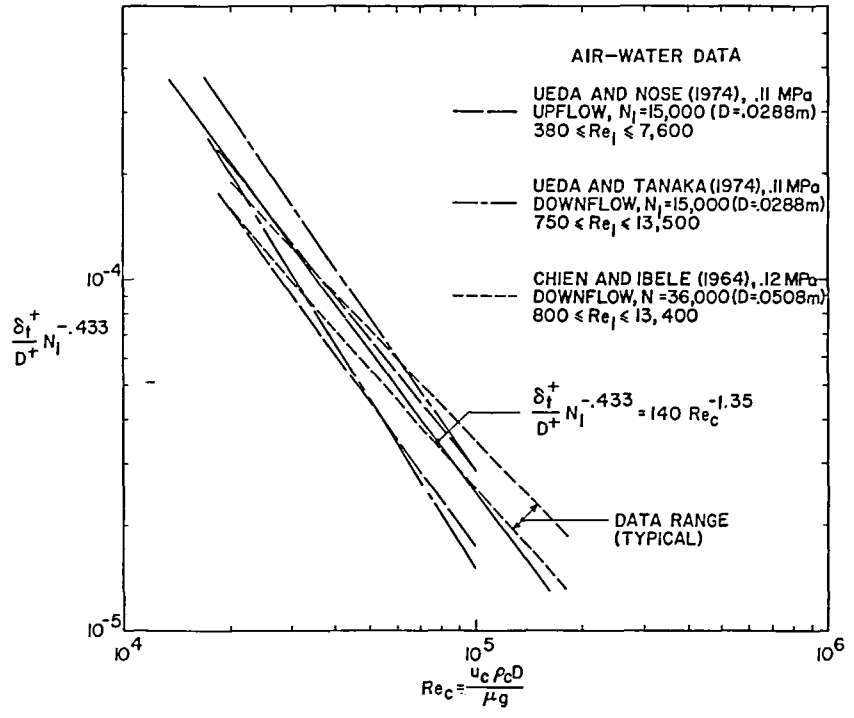

FIG. 2. Continuous liquid layer thickness representation.

and that δ_t can be regarded as a form of the boundary layer thickness for the liquid film. In this sense, the representation (19) is similar to the boundary layer thickness representation in single phase external flows. Equation (19) shows that at low values of the liquid–gas interface shear stress (low Re_c), δ_t exceeds the film thickness δ. In such a case, the liquid film acquires a falling film turbulence structure in which the velocity profile is fully determined by the universal velocity profile. The experimental data [4] for falling liquid films appear to confirm the general validity of this profile.

The wavy layer thickness $(\delta_c - \delta_t)$ was measured by Ueda and Tanaka [4] in downflow, and by Ueda and Nose [5] in upflow. This thickness depends on the gas as well as on the liquid film Reynolds numbers. $(\delta_c - \delta_t)$ increases with the gas velocity and with the film Reynolds number as the wave structure changes from smooth- to 3-dim. to roll wave pattern. It becomes a maximum at the point of breakdown of roll waves and at the onset of the annular-mist flow. Beyond the annular–annular-mist flow transition point, the wavy layer thickness decreases. At low gas velocities the height of the wave crests is considerably higher in upflow than in downflow.

From the above discussion, it is clear that the thickness of the wavy layer is a complex function of the topological structure of the flow field, and the wavy layer effective momentum diffusivity representation in equation (4) does not appear to be simple. To by-pass this difficulty, it is evident from Fig. 1 that it is reasonable to postulate that $(\delta_c - \delta_t) = O(\delta - \delta_t)$, and thus seek a relation for the wavy layer effective momentum diffusivity in the following form:

$$(\mu_{eff}/\mu_l)_{wl} = f_3(\delta^+ - \delta_t^+). \tag{20}$$

Figure 3 illustrates the relationship (20) where $(\mu_{eff}/\mu_l)_{wl}$ was computed from equation (15) and δ_t^+ from equation (19) by utilizing the experimental data of Chien and Ibele [3], and Ueda *et al.* [4, 5] for W^+, δ^+, τ_i/τ_w, Re_c, N_l and D^+. The data in the figure are reasonably well represented by the following equation:

$$(\mu_{eff}/\mu_l)_{wl} = 1 + C_1(\delta^+ - \delta_t^+)^n \tag{21}$$

where $C_1 = 1.6 \times 10^{-3}$ and $n = 1.8$. Equation (21) is valid for a wide range of film and gas Reynolds numbers, different tube diameters, and for upflow and downflow flow configurations.

The scatter of data points in Fig. 3 reflects the uncertainty of the experimental data and the postulate of the validity of the universal velocity profile in the continuous layer region of the liquid film as well as the neglect of the second order effects in the representation for the effective diffusivity in equation (20). This data scatter is not very significant. At low values of $(\delta^+ - \delta_t^+)$, equation (21) is probably not accurate since, as previously noted, the experimental data are lacking for the exact distribution of δ_t^+. In Fig. 2, this region corresponds to $Re_c < 1.5 \times 10^4$. The incomplete representation of δ_t^+ at low values of Re_c should lead to the overprediction in heat transfer rate through the liquid film due to the underestimation of the wavy layer thermal resistance. That is, at low Re_c the theory overpredicts δ_t^+ due to the lack of experimental data on the distribution of δ_t^+. This in turn underpredicts the wavy layer thickness and overpredicts the turbulence intensity in the film, and thus overpredicts the heat transfer rate.

Equations (15), (19) and (21) allow a solution for the film thickness distribution as a function of the film Reynolds number if the expressions for Re_c, τ_i/τ_w and

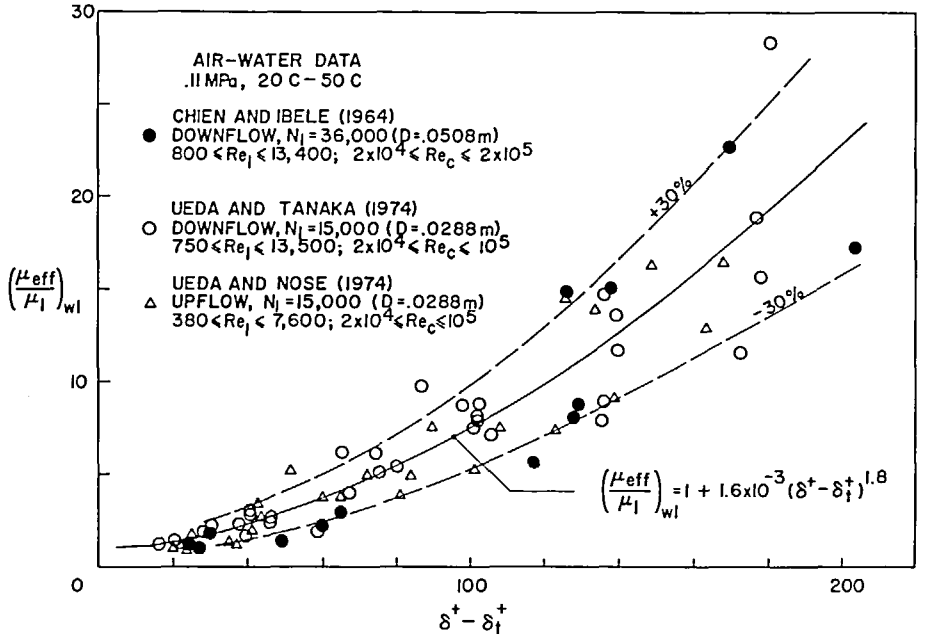

FIG. 3. Wavy layer effective diffusivity.

D^+ are known. These expressions are not all independent and their relationship is discussed below.

2.5. *Hydrodynamics*

Neglecting (1) the liquid film and gas core inertia effects, (2) mass transfer through the liquid film–gas core interface, and (3) assuming that the gas core contains liquid droplets in a homogeneous flow, it is possible to eliminate the pressure gradient between the momentum equation for the two-phase mixture and a momentum equation for the liquid film to obtain [16]

$$\frac{\tau_i}{\tau_w}=\left(1-\frac{2\delta^+}{D^+}\right)\left[1-\oplus\alpha_c\left(1-\frac{\delta^+}{D^+}\right)\left(\frac{N_l^2}{D^{+3}}\right)\delta^+\right]. \tag{22}$$

$\alpha_c = A_g/(A_g+A_d)$ is the core void fraction, A_g is the area of the core which is occupied by the gas, A_d is the area of the core which is occupied by liquid droplets, $D^+ = \rho_l D u^*/\mu_l$, and N_l is the two-phase Grashof number defined above. The symbol $\oplus$ in equation (22) is equal to + for downflow, − for upflow, and is equal to zero for horizontal flow. If the interfacial shear stress parameter β (defined first by Dukler [6] and equal to τ_i^* in refs. [4, 5, 11] is defined by the relation

$$\beta \equiv \frac{|\tau_i|}{[g^2(\rho_l-\rho_g)\mu_l^2]^{1/3}}=\frac{\tau_i}{\tau_w}\left(\frac{D^{+3}}{N_l^2}\right)^{2/3} Bo^{1/3} \tag{23}$$

where $Bo = 1-\rho_g/\rho_l$ is the buoyancy number, then equation (22) is reduced to

$$\oplus\alpha_c\left(1-\frac{\delta^+}{D^+}\right)\left(\frac{N_l^2}{D^{+3}}\right)\delta^+ + \beta\frac{\left(\frac{N_l^2}{D^{+3}}\right)^{2/3}}{Bo^{1/3}\left(1-\frac{2\delta^+}{D^+}\right)}-1=0. \tag{24}$$

Equation (24) is similar to the formulations of Dukler [6] and Hewitt [7] if it is assumed that $\alpha_c = 1$, $\delta^+/D^+ \ll 1$ and $Bo \cong 1$.

The Reynolds number, Re_c, can be related to the interfacial shear stress parameter β, core void fraction α_c, buoyancy number Bo, two-phase Grashof number N_l, and to the ratio of liquid and gas viscosities. This relationship follows from the well-known expression for the interfacial friction factor in annular flow [18], i.e.

$$f_i \equiv \frac{\tau_i}{\frac{1}{2}\rho_c u_c|u_c|}=0.079\,Re_c^{-1/4}\left(1+300\frac{\delta^+}{D^+}\right). \tag{25}$$

Using equation (23), and the definitions of $Re_c = u_c\rho_c D/\mu_g$ and $\rho_c = \rho_g\alpha_c+\rho_l(1-\alpha_c)$, the above equation becomes

$$Re_c=\left\{\frac{\mu_l}{\mu_g}N_l^{2/3}\left[\frac{2\beta(1-Bo)\left(\alpha_c+\frac{1-\alpha_c}{1-Bo}\right)}{0.079\left(1+300\frac{\delta^+}{D^+}\right)Bo^{1/3}}\right]^{1/2}\right\}^{8/7} \tag{26}$$

The void fraction α_c can be expressed in terms of the liquid entrainment in the core [16] which in turn can be expressed in terms of the interfacial shear stress and film thickness [18]. For the present purpose, however, I will treat α_c as an independent variable to simplify the theory. (It is shown below in the discussion for vertical upflow that the value of $\alpha_c \neq 1$ is in better accord with the experiment than a value of $\alpha_c = 1$.)

Equations (15), (19), (21), (24), and (26) allow us to express $W^+ = W^+(\delta^+, \beta, \mu_g/\mu_l, N_l, Bo, \alpha_c)$. Figure 4 illustrates some typical solutions for (1) air–water downflow at near atmospheric pressure, (2) no entrainment of liquid droplets in the gas core, and (3) for different values of the interfacial shear parameter β and two-phase Grashof number N_l. Shown also in the same figure are the solutions utilizing the universal velocity profile throughout the liquid film and by Dukler [6]. For $\beta > 10$ these two solutions are identical.

Comparing the present analysis results with the universal velocity profile or Dukler in Fig. 4, the present analysis gives thinner liquid films, and the slope of the film thickness–Reynolds number relationship shows a steeper behavior at high film mass flow-rates. The effect of the tenfold increase in N_l is not very significant and tends to give thicker films at high Re_l. At low Re_l all solutions in Fig. 4 converge to the laminar values and no dependence on N_l is noticeable.

2.6. *Heat transfer*

In order to compare the results of the present analysis with the experimental data of heat transfer, I have developed a simple model in which the axial conduction and convection in the liquid film are neglected.

From the expression for the heat flux in the liquid film

$$q = -(k_l+\rho_l Cp_l\varepsilon_h)\frac{\partial T}{\partial y}, \tag{27}$$

and from the definition of the non-dimensional film temperature

$$T^+ \equiv \frac{Cp_l\rho_l u^*(T_w-T)}{q_w}, \tag{28}$$

the heat flux expression becomes

$$\frac{\partial T^+}{\partial y^+}\left(\frac{1}{Pr_l}+\frac{1}{Pr_{lt}}\frac{\varepsilon_m}{\nu_l}\right)=\frac{\partial T^+}{\partial y^+}\left(\frac{\mu_{eff}}{\mu_l}\right)\frac{1}{Pr_{eff}}=\frac{q}{q_w}=1. \tag{29}$$

$Pr_l = \mu_l Cp_l/k_l$ is the molecular Prandtl number, $Pr_{lt} = \varepsilon_m/\varepsilon_h$ is the turbulent Prandtl number, $Pr_{eff} = \mu_{eff}/\rho_l\varepsilon_{eff}$ is the effective Prandtl number, and ε_m and ε_h are turbulent momentum and heat diffusivities, respectively.

For

$$y^+ \leqslant \delta_t^+ \leqslant 5, \quad \varepsilon_m/\nu_l = 0, \tag{30}$$

$$5 < y^+ \leqslant \delta_t^+ \leqslant 30, \quad \varepsilon_m/\nu_l = y^+/5-1, \tag{31}$$

$$30 < y^+ \leqslant \delta_t^+, \quad \varepsilon_m/\nu_l = y^+/2.5-1, \tag{32}$$

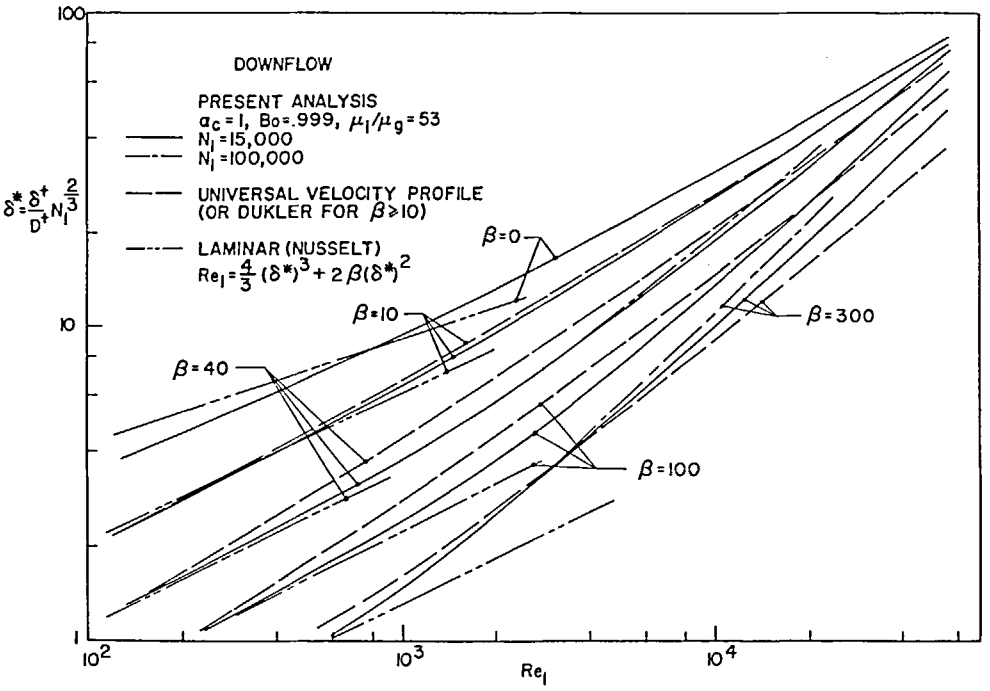

FIG. 4. Liquid film thickness distribution in downflow.

$\delta_t^+ < y^+ \leqslant \delta^+$,

$$(\mu_{eff}/\mu_l)_{wl} = 1 + 1.6 \times 10^{-3}(\delta^+ - \delta_t^+)^{1.8}. \quad (33)$$

Substituting equations (30)–(33) into equation (29), the temperature distribution in the film was obtained, and the Nusselt number was computed from the following:

$$Nu_\delta = \frac{q_w \delta}{(T_w - T)k_l} = \frac{Pr_l \delta^+}{T^+}. \quad (34)$$

The above heat transfer formulation utilizes molecular and turbulent Prandtl numbers in the continuous region of the liquid film, and an effective Prandtl number in the wavy layer region of the film. It is not clear to me that the wavy layer region effective diffusivity should be divided into molecular and turbulent liquid parts, since this diffusivity represents the states of both liquid and gas phases. Equation (33) should be viewed as an expression for the *two-phase* diffusivity. Using an effective Prandtl number to represent the transport of heat in this region appears to be reasonable.

Figure 5 compares the heat transfer results from the present analysis with the results of the universal velocity profile for downflow with T^+ in equation (34) evaluated at δ^+. At low Re_l, the two analyses give identical results, but at Re_l from 10^3 to 10^4, the present analysis gives lower heat transfer coefficients by up to 50%. Above $Re_l = 2 \times 10^4$ and for very high β, the validity of the present results is uncertain due to the lack of experimental data to confirm the validity of equation (19). Higher values of N_l tend to give higher heat transfer coefficients which is reasonable, since high N_l also implies larger tube diameters and thus a larger area for the heat transfer.

Comparing the heat transfer results of the present analysis in upflow with the predictions of the universal velocity profile and the analysis of Hewitt [7], also shows lower heat transfer coefficients. The steam–water upflow experimental data of Collier *et al.* [19] in an annulus show that the analysis of Hewitt [7] overpredicts the experimental heat transfer coefficients by up to 50%, and hence confirm the correct trend of the present theory.

A possible reason why the analyses of Dukler, Hewitt and the universal velocity profile overpredict the heat transfer rate is that they overestimate the turbulence intensity of the film in the wavy layer region. For example, at typical values of $\delta_t^+ = 15$ and $y^+ = 100$, equation (32) gives $\mu_{eff}/\mu_l = 40$, and equation (33) gives $\mu_{eff}/\mu_l = 6$. The low values of the wavy layer effective diffusivity for momentum clearly show that the turbulence of waves is not very effective for momentum and heat transport as it has been often assumed in the past.

3. DISCUSSION

In order to assess the range of validity of the proposed theoretical model, it is necessary to test the model against the experimental data in different flow configurations. This is presented below, whereas the design curves will be presented elsewhere.

3.1. *Vertical downflow*

The distribution of liquid film thickness vs the film Reynolds number is compared in Fig. 6 with the experimental data of Chien and Ibele [3], and Ueda and

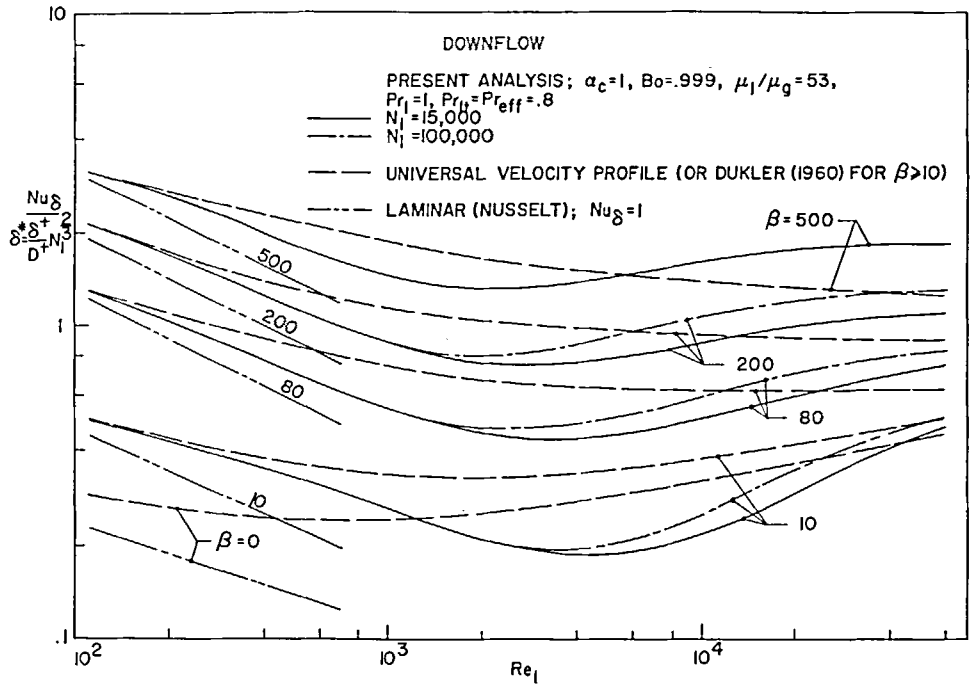

FIG. 5. Heat transfer distribution in the liquid film in downflow.

Tanaka [4]. The present analysis reproduces the experimental data very well, and at high film Reynolds numbers the data exhibit slightly larger slopes than the analytic results.

Heat transfer results with $Pr_{lt} = 0.8$ and $Pr_{eff} = 0.5$ are compared with the experimental data in Fig. 7 where the Nusselt number was computed by utilizing the film bulk temperature,

$$T_b^+ = \left(\int_0^{\delta^+} T^+ u^+ \, dy^+ \right) \Big/ W^+,$$

in equation (34). Changing Pr_{eff} to 0.8 gives slightly lower heat transfer coefficients, and with $Pr_{lt} = Pr_{eff} = 1$ the theory underpredicts the heat transfer rate in the

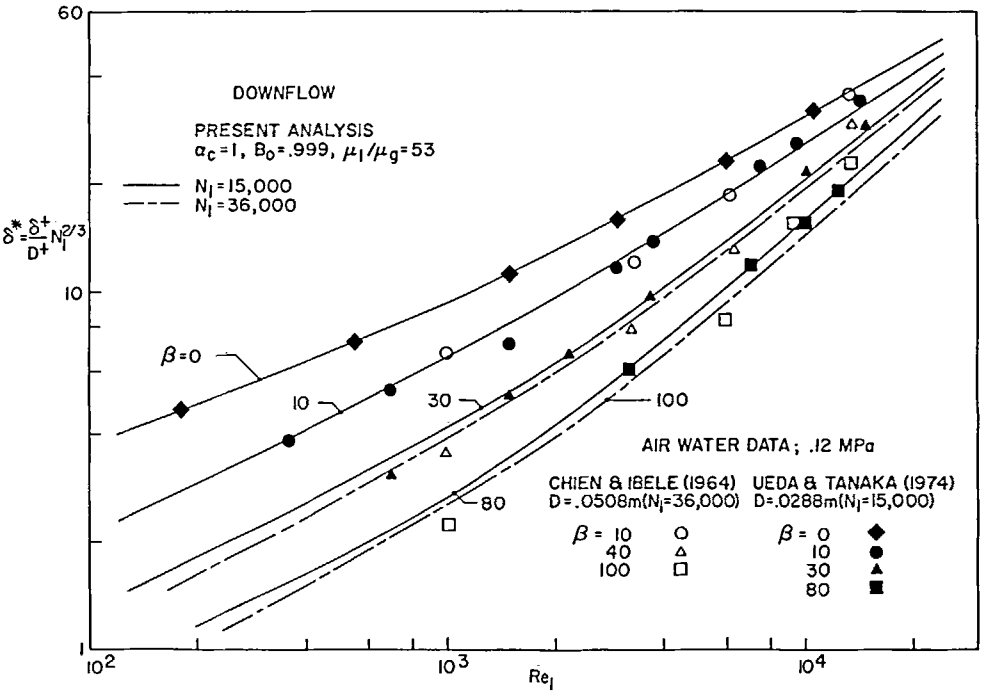

FIG. 6. Film thickness in downflow and comparison with the experimental data.

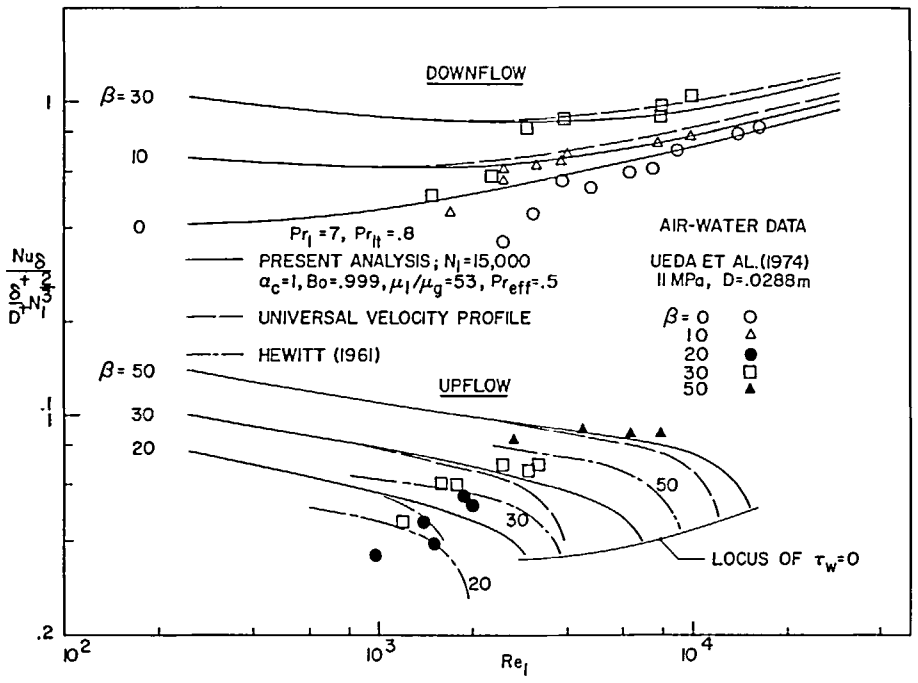

FIG. 7. Heat transfer in upflow and downflow, and comparison with the experimental data.

turbulent film flow regime by 10%. For $Re_l > 3000$, the agreement between the present analysis and the experiment is very good, and there is about 10% difference in prediction utilizing the universal velocity profile. For $Re_l < 3000$ the experimental data fall below the theoretical results, and the disagreement is worse at lower β. The causes for this disagreement are the neglect of convection energy transport in the film and the underestimate of the wavy layer thermal resistance. The latter is probably more important and clearly points to the need for improvement of the continuous liquid layer thickness representation δ_l^+ in equation (19) at low Re_c.

3.2. *Vertical upflow*

The hydrodynamic results for upflow are compared with the experimental data for air and water in Fig. 8. The present analysis reproduces the experiment better than the analysis of Hewitt [7] and the analysis using the universal velocity profile. The present analysis fails, however, to reproduce the experiment close to the locus of zero value of the wall shear stress. This is of no surprise, since the fundamental hypothesis in the paper on the structure of turbulence in the liquid film is violated in the neighborhood of $\tau_w = 0$. At high values of the interfacial shear parameter β in Fig. 8, the experimental data show a shift towards the left of the analytic curves. Within the scope of the present theory it is possible to explain this shift by the effect of droplet entrainment in the gas core. A value of $\alpha_c = 0.999$ (which amounts to 0.1% of the gas core area being occupied by liquid droplets) is sufficient to bring into agreement the analysis and the experiment as shown in Fig. 8. Higher droplet entrainment in upflow than in downflow was experimentally confirmed by Ueda and Nose [5] among others.

Heat transfer results and data for the air–water upflow are illustrated in Fig. 7. Although the agreement is good between the present analysis and the experimental data at higher values of the interfacial shear parameter β and film Reynolds numbers, this agreement is not as satisfactory at low β and for Re_l less than 2000. The inclusion of liquid film convection effect into the heat transfer model should improve the analytic prediction. The results from the present analysis agree better with the experimental data than do the results from the analyses of Hewitt and the universal profile.

3.3. *Horizontal flow*

The basic turbulence model for the liquid film is tested in Figs. 9 and 10 against the experimental data [8] for air and water in horizontal stratified flow. W^+ and Nu_δ from the theory were computed from equations (15), (19), (21), and (34) by utilizing the experimental values for δ^+, τ_i/τ_w, Re_c and by computing D^+ on the basis of the rectangular channel hydraulic diameter. Nu_δ in Fig. 10 is based on the film bulk temperature.

At high film Reynolds numbers in Fig. 9, the present theory overpredicts the experimental film mass flow-rate by 10%, and at lower Re_l the theory is in a very good accord with the experimental data. These facts dramatically illustrate the similarity of the liquid film structure in different flow orientations.

The heat transfer results from the theory shown in

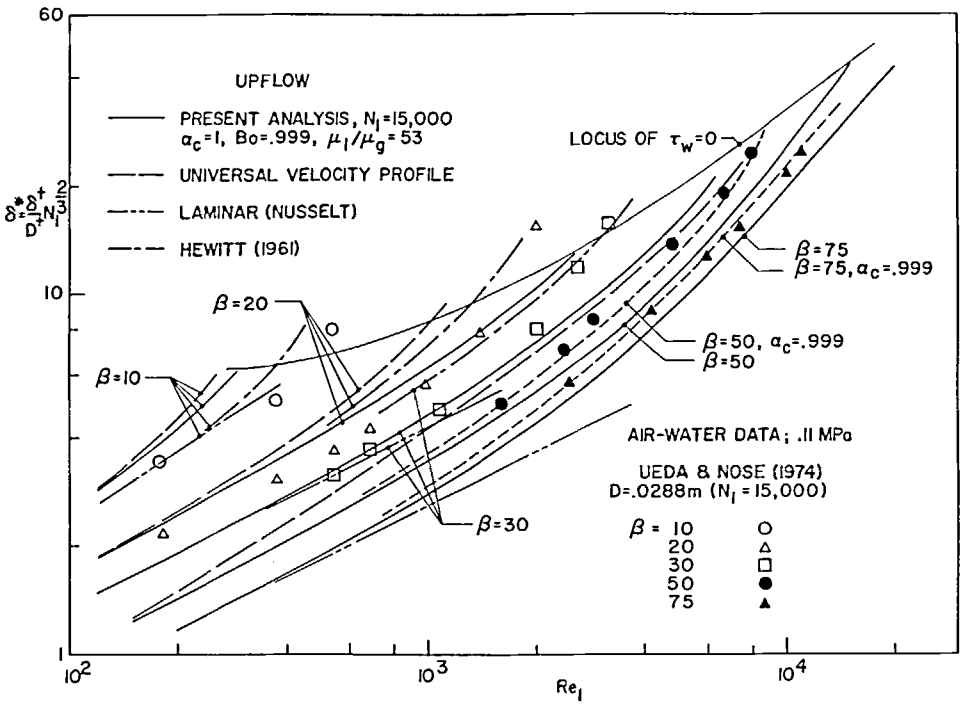

FIG. 8. Film thickness in upflow and comparison with the experimental data.

Fig. 10 were computed using $Pr_{lt} = 0.8$ and $Pr_{eff} = 0.5$, and the difference in results is very small if it is chosen that $Pr_{eff} = 0.8$. In the roll waves flow regime, the predicted Nusselt numbers are on the average slightly higher than for the 3-dim. flow regime. Although this difference is small, it nevertheless illustrates the need to further improve the turbulence structure in the wavy layer region of the film. In the smooth interface flow regime or for $Re_l < 2000$, the present analysis overestimates the heat transfer. This is primarily due to

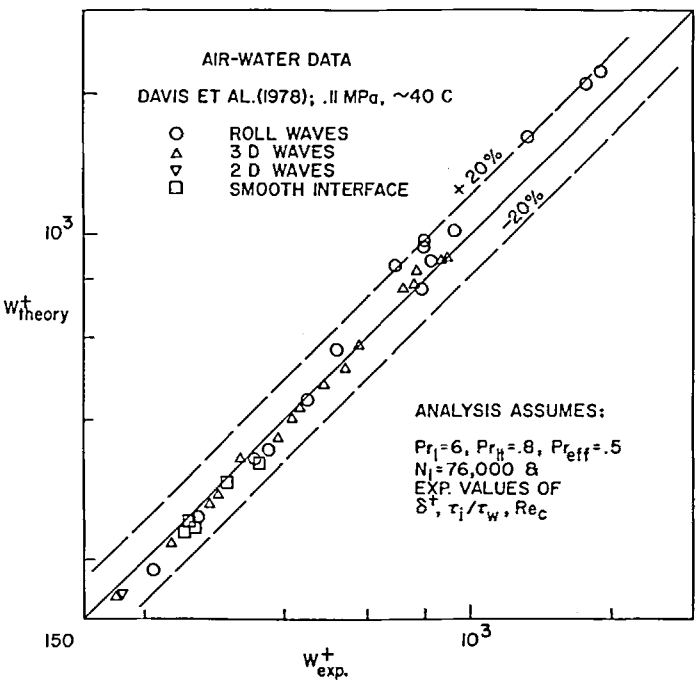

FIG. 9. Comparison between the predicted and experimental values of liquid flow-rates in a horizontal stratified flow.

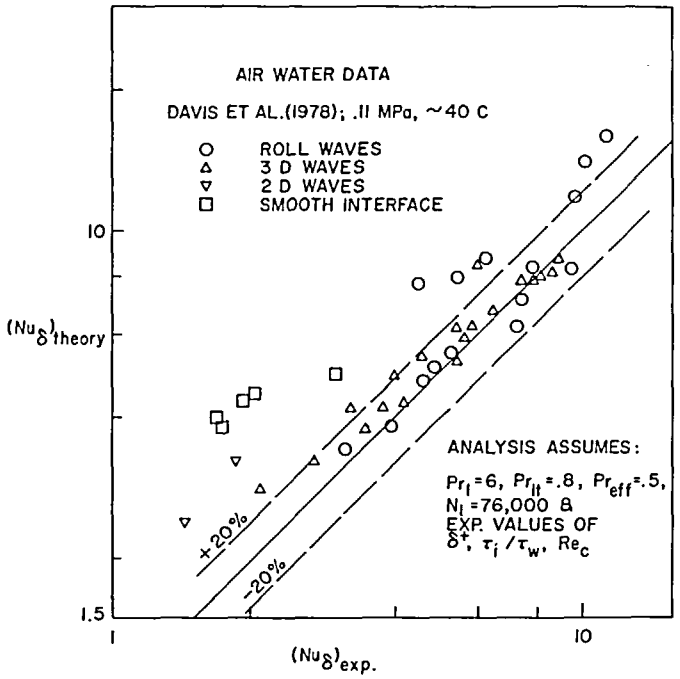

FIG. 10. Comparison between the predicted and experimental values of Nusselt numbers in a horizontal stratified flow.

the underestimation of the wavy layer thermal resistance.

The horizontal annular flow usually involves large variations in the average film thickness around the periphery of the tube as shown by Cheremisinoff and Davis [20]. In this case, the present analysis should be applied locally at each peripheral position of the tube, and the total flow and heat transfer can then be calculated by integration around the tube.

3.4. *Condensing flow in a vertical tube*

The low subcooling number experimental data of Ueda *et al.* [15] are illustrated in Fig. 11 together with the prediction utilizing the present analysis and analysis with the universal velocity profile. The agreement of film thickness vs film Reynolds number distribution between the present analysis and the experiment is excellent. Heat transfer results in Fig. 11 from the present analysis reproduce the experimental data for $Re_l > 2000$ very well and up to 50% better than the analysis of the universal velocity profile. For $Re_l < 2000$, the agreement between theory and experiment is less satisfactory, and at $Re_l = 1000$ the disagreement is 50% at low β. At high β the theory only slightly overpredicts the experimental heat transfer coefficients.

It is apparent that future efforts to improve the theory must direct their attention to the transition zone from $Re_l = 500$ to $Re_l = 2000$ where the present theory underestimates the wavy layer thermal resistance. At the present time, a reasonable design procedure might be to locate the points of minimum on the present analysis heat transfer curves in Fig. 11 and draw horizontal lines to the laminar solution curves. The experimental data appear to follow this path reasonably well.

4. SUMMARY AND CONCLUSIONS

The division of liquid film in the two-phase annular flow into continuous and wavy layer regions is a basic experimental fact. In the paper, the two-layer liquid film structure was considered by assuming the validity of the single phase turbulence structure in the continuous layer and by modifying the single phase structure of turbulence in the wavy layer region of the film. Experimental data confirmed the validity of this basic assumption and revealed the values for the wavy layer momentum diffusivity.

The two-layer liquid film model was incorporated into an analysis for the prediction of hydrodynamics and heat transfer in annular flow, and extensive comparison of the theory with the experimental data was made in upflow, downflow, and horizontal two-phase annular flows. The theoretical model gives substantial improvement in hydrodynamics and heat transfer over existing theories and is simpler to use. Comparison of the analysis with the experimental data at high Prandtl numbers shows that in the continuous layer region of the liquid film the turbulent Prandtl number has a value between 0.8 and 1, and in the wavy layer region of the film the effective Prandtl number has a value close to 0.5. The low value of Pr_{eff} in the wavy layer region implies that the heat transport process is not very effective to, or from, the continuous layer. Stated differently, the waves transfer their heat energy over distances which are larger than the thickness of the wavy layer.

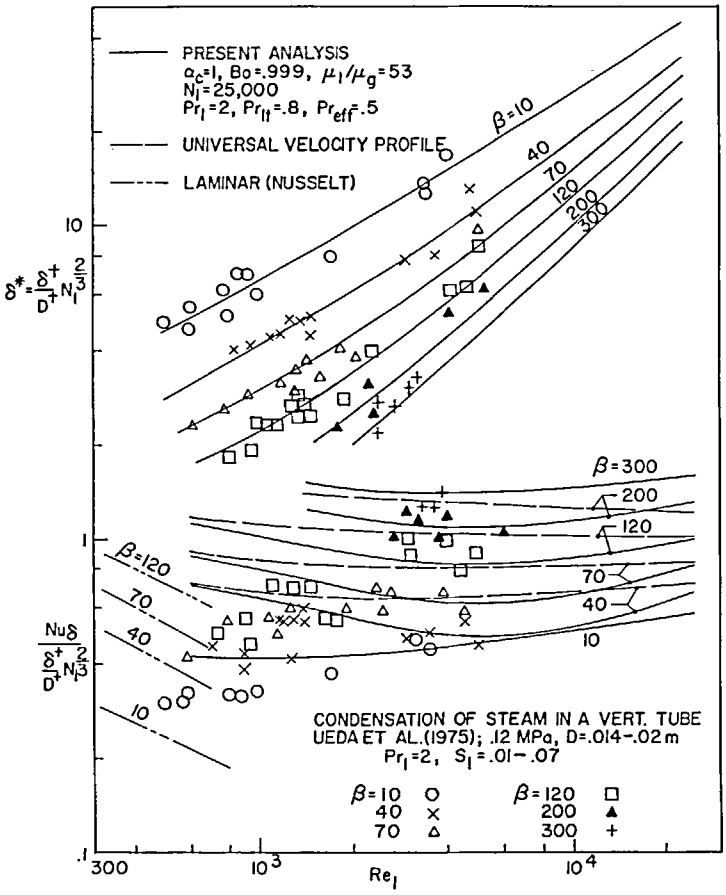

FIG. 11. Comparison of analysis with the condensation of stream data.

Further work is required to determine the continuous liquid layer thickness distribution at low and very high gas and liquid film velocities, and to isolate any secondary effects in the distribution of δ_l in different flow orientations. For $Re_l < 2000$, the heat transfer analysis needs to include convective energy transport in the liquid film in order to assess its importance.

REFERENCES

1. D. P. Frisk and E. J. Davis, The enhancement of heat transfer by waves in stratified gas–liquid flow, *Int. J. Heat Mass Transfer* **15**, 1537–1551 (1972).
2. A. E. Dukler, Characterization, effects and modeling of the wavy layer gas–liquid interface, in *Progress in Heat and Mass Transfer*, Vol. 6, pp. 207–234. Pergamon Press, New York (1972).
3. S. Chien and W. Ibele, Pressure drop and liquid film thickness of two-phase annular and annular-mist flows, *Trans. Am. Soc. Mech. Engrs*, Series C, *J. Heat Transfer* **86**, 80–96 (1964).
4. T. Ueda and T. Tanaka, Studies of liquid film flow in two-phase annular and annular-mist flow regions; Part 1, Downflow in a vertical tube, *Bull. Japan. Soc. Mech. Engrs* **17**, 603–613 (1974).
5. T. Ueda and S. Nose, Studies of liquid film flow in two-phase annular and annular-mist flow regions; Part 2, Upflow in a vertical tube, *Bull. Japan. Soc. Mech. Engrs* **17**, 614–624 (1974).
6. A. E. Dukler, Fluid mechanics and heat transfer in vertical falling-film systems, *Chem. Engng Prog. Symp. Ser.* **56**, 1–10 (1960).
7. G. F. Hewitt, Analysis of annular two-phase flow; Application of the Dukler analysis to vertical flow in a tube, UKAEA Rep. AERE-R-3690 (1961).
8. E. J. Davis, N. P. Cheremisinoff and G. Sambasivan, Heat and momentum transfer analogies for two-phase transfer stratified and annular flows, in *Two-Phase Transport and Reactor Safety*, Vol. 2, pp. 577–608. Hemisphere, New York (1978).
9. W. P. Goss, K. Kammula and R. W. Zub, An integral technique for predicting wall and interfacial shear stress in turbulent condensing annular-mist flow, in *Proc. 6th Int. Heat Transfer Conf.*, pp. 425–430. Hemisphere, New York (1978).
10. D. Butterworth, An analysis of film flow and its application to condensation in a horizontal tube, *Int. J. Multiphase Flow* **1**, 671–682 (1974).
11. F. Blangetti and E. U. Schlunder, Local heat transfer coefficients on condensation in a vertical tube, in *Proc. 6th Int. Heat Transfer Conf.*, Vol. 2, pp. 437–442. Hemisphere, New York (1978).
12. V. Levich, *Physicochemical Hydrodynamics*. Prentice Hall, New Jersey (1962).
13. J. C. Jepsen, O. K. Crosser and R. H. Perry, The effects of wave induced turbulence on the rate of absorption of gases in falling liquid film, *A.I.Ch.E. Jl* **12**, 192–196 (1966).
14. D. Butterworth and G. F. Hewitt, *Two-Phase Flow and Heat Transfer*. Oxford University Press (1977).
15. T. Ueda, T. Kubo and M. Inoue, Heat transfer for steam condensing inside a vertical tube, in *Proc. 5th Int. Heat*

Transfer Conf., Vol. 3, pp. 304–308. Hemisphere, New York (1976).
16. F. Dobran, Condensation heat transfer and flooding in a counter-current subcooled liquid and saturated vapor flow, in *Thermal Hydraulics in Nuclear Power Technology*, pp. 9–19. ASME, New York (1981).
17. G. B. Wallis, *One-Dimensional Two-Phase Flow*. McGraw-Hill, New York (1969).
18. A. E. Bergles, J. G. Collier, J. M. Delhaye, G. F. Hewitt and F. Mayinger, *Two-Phase Flow and Heat Transfer in Power and Process Industries*. Hemisphere, New York (1981).
19. J. G. Collier, P. M. C. Lacey and D. J. Pulling, Heat transfer to two-phase gas–liquid systems, *Trans. Inst. Chem. Engrs* **42**, 114–121 (1964).
20. N. P. Cheremisinoff and E. J. Davis, Stratified turbulent–turbulent gas–liquid flow, *A.I.Ch.E. Jl* **25**, 48–56 (1979).

ANALYSE HYDRODYNAMIQUE ET THERMIQUE D'UN ECOULEMENT ANNULAIRE DIPHASIQUE AVEC UN NOUVEAU MODELE DE TURBULENCE DE FILM LIQUIDE

Résumé—On présente une nouvelle méthode d'analyse des écoulements annulaires diphasiques avec films liquides turbulents. A partir de l'observation expérimentale, le film liquide est divisé en une couche continue adjacente à la surface du canal et en une autre couche agitée proche de l'interface liquide–gaz. Dans la région de la couche continue de film, on suppose que la structure de la turbulence est semblable à celle d'un écoulement monophasique dans un tuyau, et dans l'autre couche du film, on suppose que la longueur de la diffusion turbulente est proportionnelle à l'épaisseur de cette région. Des expériences d'écoulement ascendants et descendants confirment la validité de l'hypothèse sur la structure turbulente du film et donnent la valeur de la diffusivité de la quantité de mouvement dans la couche agitée. Cette diffusivité a une valeur plus basse que dans l'écoulement monophasique dans un tube à des distances équivalentes de la paroi du canal. La structure bidimensionnelle du film liquide est intégrée dans l'analyse des écoulements annulaires diphasiques. Des résultats analytiques sont comparés à ceux d'autres modèles et à des données expérimentales pour des écoulements ascendant, descendant et horizontal. Dans tous les cas considérés, une très bonne comparaison est réalisée aussi bien pour l'hydrodynamique que pour le transfert thermique.

BESCHREIBUNG DER HYDRODYNAMIK UND DES WÄRMETRANSPORTS BEI ZWEIPHASIGER RINGSTRÖMUNG MIT HILFE EINES NEUEN TURBULENTEN FLÜSSIGKEITSFILMMODELLS

Zusammenfassung—Eine neue Methode zur Beschreibung der Hydrodynamik und des Wärmetransports bei zweiphasiger Ringströmung mit turbulentem Flüssigkeitsfilm wird vorgestellt. Der Flüssigkeitsfilm der zweiphasigen Ringströmung wird, auf experimentellen Beobachtungen beruhend, in eine zusammenhängende, an der Kanalwand haftende Schicht und in eine wellige Schicht an der Grenzfläche Flüssigkeit/Gas eingeteilt. Es wird angenommen, daß im Bereich der zusammenhängenden Flüssigkeitsschicht des Films die turbulente Struktur gleich der einer turbulenten einphasigen Rohrströmung ist. Im Bereich der welligen Schicht des Films wird angenommen, daß die Scheindiffusionslänge proportional zur Dicke dieser Schicht ist. Messungen bei Aufwärts- und Abwärtsströmung erhärteten die Stichhaltigkeit der grundlegenden Annahmen über die Turbulenzstruktur im Film und lieferten den Wert des Impulsaustausch-Koeffizienten der welligen Schicht. Es zeigte sich, daß dieser Austausch-Koeffizient bei gleichem Abstand von der Kanalwand einen kleineren Wert als bei einphasiger Rohrströmung besitzt. Die Zweischichtenstruktur des Flüssigkeitsfilms wurde in eine Berechnungsmethode der Strömungsvorgänge und des Wärmetransports bei zweiphasiger Ringströmung eingebracht. Die analytischen Ergebnisse werden mit denen anderer analytischer Modelle und den Meßergebnissen bei Aufwärts-, Abwärts- und horizontaler Strömung verglichen. In allen untersuchten Fällen konnte eine sehr gute Übereinstimmung, sowohl bei den Strömungsvorgängen als auch im Wärmetransport festgestellt werden.

АНАЛИЗ ГИДРОДИНАМИКИ И ТЕПЛОПЕРЕНОСА ДВУХФАЗНОГО КОЛЬЦЕВОГО ТЕЧЕНИЯ С ПОМОЩЬЮ НОВОЙ МОДЕЛИ ТУРБУЛЕНТНОЙ ЖИДКОСТНОЙ ПЛЕНКИ

Аннотация—Предложен новый метод анализа гйдродинамики и теплопереноса двухфазных кольцевых турбулентных течений. Из наблюдений в опытах установлено, что жидкостную пленку при двухфазном кольцевом течении в канале можно подразделить на непрерывный пристеночный слой и волновой, примыкающий к границе раздела жидкость–газ. Для области непрерывного слоя пленки турбулентная структура принимается аналогичной структуре однофазного турбулентного потока в трубе, а в волновой области—длина участка с вихревой диффузией полагается пропорциональной толщине этой зоны. Измеренные вверх и вниз по потоку характеристики подтверждают справедливость основного предположения о турбулентной структуре пленки и позволяют определить значение коэффициента вихревой вязкости волнового слоя. В этом случае коэффициент более низкий, чем при однофазном течении в трубе на тех же расстояниях от стенки канала. Структура двухслойной жидкостной пленки используется для расчета гидродинамики и теплопереноса при кольцевых двухфазных течениях. Проведено сравнение полученных расчетами результатов с предсказаниями по другим аналитическим моделям и опытными данными для восходящих, нисходящих и горизонтальных потоков. Во всех рассмотренных случаях получено хорошее совпадение как данных по гидродинамике, так и теплопереносу.